Short-time Maximum Entropy Method Analysis of Molecular Dynamics Simulation: Unimolecular Decomposition of Formic Acid

Osamu Takahashi, Tetsuo Nomura, Kiyohiko Tabayashi, and Katsuyoshi Yamasaki*

Department of Chemistry, Hiroshima University, Higashi-Hiroshima 739-8526, Japan

Abstract

We performed spectral analysis by using the maximum entropy method instead of the traditional Fourier transform technique to investigate the short-time behavior in molecular systems, such as the energy transfer between vibrational modes and chemical reactions. This procedure was applied to direct ab initio molecular dynamics calculations for the decomposition of formic acid. More reactive trajectories of dehydrolation than those of decarboxylation were obtained for Z-formic acid, which was consistent with the prediction of previous theoretical and experimental studies. Short-time maximum entropy method

analyses were performed for typical reactive and nonreactive trajectories. Spectrograms of a reactive trajectory were obtained; these clearly showed the reactant, transient, and product regions, especially for the dehydrolation path.

Keywords: Classical trajectory calculation; Short-time Fourier transformation; Maximum entropy method; Spectrogram; Formic acid

1. Introduction

Dynamical processes within the order of femtoseconds (fs) in molecular systems are of interest to researchers in the field of chemical physics and physical chemistry because bond breaking and vibrational energy redistribution in a molecule are observed on this time scale [1]. In order to understand these phenomena better, fs or sub-fs laser spectroscopy [2] and X-ray photoelectron spectroscopy [3,4], which reflect the decay process following the core-excitation as atomic motion within a core-hole lifetime of several fs, have been developed.

Theoretically, molecular dynamics (MD) simulations have been useful and widely applied to simulate the dynamics of a polyatomic system. Recently, it has become common to calculate the potential energies and forces step-by-step using ab initio molecular orbital (MO) calculations and to examine the dynamical process of a chemical reaction; this process is called the “ab initio MD” or the “direct ab initio” method. In order to

characterize the dynamical features of MD simulations, a power spectral analysis by Fourier transformation (FT) of either the coordinates or the auto-correlation functions of dynamical variables such as the coordinates and velocities has been widely used [5-7]. Furthermore, the short-time FT (ST-FT) technique has been successfully used to describe the chemical reaction [8-11]. For other procedures, wavelet transform techniques have recently been developed to examine the short-time dynamics in a molecule [12,13]. In the present paper, we have developed the power spectral analysis by using the maximum entropy method (MEM) [14-17] instead of the ordinary FT technique. MEM can produce a power spectrum by using the short-time trajectory information of several vibrational periods. Furthermore, by combining MEM with the ST-FT technique, the peak positions with time can be examined in the order of fs.

For a test case, the direct ab initio method was applied to examine the decomposition of formic acid. Many experimental [18-23] and theoretical [24-36] investigations have been reported on the thermal decomposition of formic acid. The two dissociation paths for formic acid are as follows:

$$HCOOH \rightarrow H_2O + CO \qquad (1)$$

$$\rightarrow H_2 + CO_2. \qquad (2)$$

In the previous shock tube study, it was found that the rates of these two competing paths differed substantially by around 20 - 35 times; this difference in rate was attributed to the entropy difference between the reactant and the transition state [23].

In the present paper, we show classical trajectory calculations for formic acid by using the ab initio MO method and discuss the reaction dynamics in detail by combining the ST-FT technique with MEM.

2. Computational Procedure

In order to discuss the chemical reactivity, trajectory calculations were performed for the target molecule (formic acid) by changing the initial conditions, i.e., the geometries and velocities of each atom. Initially, the classical trajectory calculations were performed for Z- and E-formic acids, which have only the zero-point energy (21.5 kcal mol^{-1} and 21.2 kcal mol^{-1} for Z- and E-formic acid, respectively). Then, Hamilton's equation of motion was integrated with a step size of 0.5 fs by using a fourth-order symplectic integrator [37], and the trajectory calculations were followed over a time period of 1.0 ps. A symplectic integrator is a numerical integration scheme for Hamiltonian systems that conserves the symplectic two-form $dp \wedge dq$ exactly, so that $(q(0),p(0)) \rightarrow (q(t),p(t))$ is a canonical transformation. This algorithm is accurate and has no accumulation of numerical errors for the total energy in contrast to the other common algorithms used for solving Hamilton's equation of motion [38]. From these calculations, 60 geometries were selected randomly. The normal mode vectors of each isomer were selected for the nine independent directions. Next, trajectory calculations were performed by adding the potential barrier and the excess energy as the kinetic energy of the molecule to one of the normal vibrational modes (ν_1 --

ν_9); the subscript of each normal mode refers to a sorted vibrational frequency in small order. E_{exc} is the excess energy that exceeds the barrier height for each path,

$$E_{exc}=E_{add}- \Delta E - E_{ZPE},$$

where E_{add} is the added kinetic energy in the molecule; ΔE, the barrier height for a path; and E_{ZPE}, the zero-point energy. The translation and rotation in the system were carefully excluded. E_{exc} was taken to be 5, 10, and 15 kcal mol^{-1} for the start geometry of both Z- and E-formic acid. Trajectory calculations were followed for a period of 1.0 ps, which was sufficient to examine the effect of the mode specific excitation. The threshold bond distance to judge that the target chemical reaction takes place was defined as R(C-O) = 3.0 Å for reaction (1) and R(C-H)=R(O-H) = 3.0 Å for reaction (2). Moreover, the final geometries were checked for each trajectory.

By using the cartesian velocities for each atom obtained from the classical trajectory calculations, power spectral analyses were performed with the MEM [14-17]. The time step of 0.5 fs was too wide to describe the sharp spectra with MEM. Fifty points were interpolated by the quadratic functions that were produced by the three nearest points.

All calculations in the present study were performed by the modified GAMESS(US) [39] using the MP2/6-31G(d,p) level of approximation.

3. Results and Discussions

3.1 Trajectory calculations from the equilibrium geometry

The relative energies of formic acid are summarized in Fig. 1. The potential energy barriers of the two decomposition paths at the MP2/6-31G(d,p) level of theory were higher than the previous values at the MP4/cc-pVQZ//B3LYP/cc-pVTZ level of theory [24]. Nevertheless, the difference in energy barriers between the two paths was comparable to the previous value; this indicated that the present computational level could be used to describe the two competing paths of formic acid decomposition. In the present study, we selected the MP2/6-31G(d,p) level for the following dynamical study.

The number of reactive trajectories per 60 runs when the equilibrium structure was considered the starting point is summarized in Table 1. As shown in Fig. 1, the relative energy between Z- and E-formic acid was 5.6 kcal mol^{-1} at the MP2/6-31G(d,p) level of theory, indicating that Z-formic acid was the main conformer at the equilibrium condition. Therefore, it can be said that in the case of Z-formic acid, many reactive trajectories produced H_2O and CO as the main products through path (1), and some trajectories produced H_2 and CO_2 as minor products through path (2). The ratio of the total reactive trajectories between them was 19.5, which is comparable with the experimental value qualitatively. The experimental ratio of the rate constant of two paths k_1/k_2 was reported as 20 - 35 at T=1400 K [23]. It should be noted that our simulations were limited to a time period within 1.0 ps, and the computational product ratio with the present scheme depended on the length of the trajectory. More reactive trajectories can be obtained for both paths by longer trajectory calculations. In order to compare the rate constants quantitatively, a greater number of trajectory calculations need to be performed by changing the initial conditions and the length of the trajectory.

Further, when a specific vibrational mode ν_8 for Z-formic acid, which corresponded to the CH stretching mode, was excited, a large number of reactive trajectories were obtained. Further for mode ν_5, no reactive trajectories were obtained. These results suggest that the reactivity differs with the excited vibrational modes. In the case of E-formic acid, many reactive trajectories were obtained for both paths because the excess energy was higher than that of Z-formic acid. It should be noted that many reactive trajectories were given to the minor products H_2 and CO_2 when mode ν_9, which was assigned to the OH stretching mode, was excited. In the case of formic acid, the chemical reaction can be accelerated by exciting a specific vibrational mode beyond the reaction barrier. These results suggest that the reactivity can be controled by exciting a specific vibrational mode and specifying the geometry.

3.2 Power spectral analysis by the maximum entropy method

In order to examine the chemical reaction of formic acid in detail, a power spectral analysis by MEM was performed. First, the comparisons between the power spectra obtained by FT and those obtained by MEM are shown in Fig. 2. The nine sharp peaks corresponded to the normal modes of formic acid, and the peak positions could also be estimated by using the frequency calculations, when the second derivative matrix of the energy with respect to the nuclear position was diagonalized at the stationary point. Some peaks obtained by FT were broadened by decreasing the window functions due to a peak

broadening by Heisenberg's uncertainty principle. On the other hand, those obtained by MEM maintained their sharpness even when a narrow window function of 250 fs was applied. Note that the number of sampling points for MEM was kept constant among these spectra by interpolating the data. The relative intensities for MEM varied with the window functions, indicating that sufficient periodic motions to describe the same spectra could not be obtained from such short trajectories. From a different viewpoint, MEM spectra could express the short-time behavior of the nuclear dynamics. It was confirmed that the peak position was identified by using a window function of 100 fs, which corresponds to several vibrational periods in the molecule. Further, it can be concluded that MEM is an effective procedure to specify the peak position of the power spectra by observing several periods of vibrational motions. An extra peak around 1700 cm^{-1} is observed in Fig. 2. This peak position was unstable for the trajectory length considered. The origin of this peak appeared to be a part of ν_7 divided by the strong coupling with the other modes, and the peak would disappear if a longer trajectory were used or many spectra were averaged with the same trajectory length.

The time propagation of the peak position could be traced by moving the window function of the MEM spectra in a long trajectory. We called this spectrum short-time MEM (ST-MEM), and a typical example is shown in Fig. 3. A window function of 500 fs was used in the spectrum, which was fairly large for the discussion in the previous paragraph. The sharpness of each vibrational mode was maintained because the added kinetic energy was not much and the vibrational mode couplings were small. Moreover, the window function for ST-MEM was so large that motions along the normal modes are enhanced. The

relative intensity fluctuated, indicating that wider window functions may be needed to obtain time-independent spectra. However, for a peak around 3800 cm^{-1}, which was assigned to the CH stretching mode, the relative intensity and peak position were maintained, suggesting that the energy transfer from this mode contributed less to the added kinetic energy.

Next, contour maps with the moving window functions are shown in Fig. 4. Such contour maps were referred to as spectrograms: the horizontal axis is the time domain (in fs), the vertical axis is the frequency domain (in cm^{-1}), and the height of the peak (the peak intensity) is expressed by a gradation from blue to red. Note that Fig. 3 and Fig. 4(a) are produced by the same trajectory. We clearly observed that the peak positions for the window function of 500 fs were mostly constant. On the other hand, the peak positions for the window function of 100 fs, especially in the range of 1000 to 2000 cm^{-1}, fluctuated largely, i.e., we observed that the vibrational modes fluctuated more when narrow window functions were used by using the ST-MEM. Our MD simulations were performed on a multi-dimensional potential energy surface. Further, it was observed that vibrational modes perturbed each other in the narrow window function of 100 fs and the peak positions shifted from those of the normal modes. We observed the fluctuation of the instantaneous vibrational frequencies by using the ST-MEM.

As suggested in Table 1, intramolecular energy vibrational redistribution is different for vibrational modes, and it is shown using the ST-MEM. Typical examples of a spectrogram after a specific mode excitation by a trajectory are shown in Fig. 5. The shape of a spectrogram differs according to the excited mode. For Fig. 5(a), the fact that strong peaks

around 1400 cm^{-1} were maintained during a period of 100 fs suggests that the energy redistribution from this mode is slow. On the other hand, for Fig. 5(b), the initial strong peaks disappeared immediately, and their intensities spread to other modes. These peak positions moved aggressively. Therefore, it was concluded that initial excited energy was diffused quickly and the memory where mode specific excitation was performed was lost within the time window of the ST-MEM.

Next, the ST-MEM for a reactive trajectory is shown in Fig. 6. Typical examples for reaction (1) and (2) are shown in Fig. 6(a) and (b), respectively. In Fig. 6(a), we observe a specific variation of a vibrational mode around 2500 cm^{-1} at the range of 100 – 500 fs, which is assigned to the CH stretching mode. It should be noted that this variation resembles that of the vibrational frequencies along the intrinsic reaction coordinate (IRC), which is shown in Fig. 2 in reference 20. Therefore, it can be concluded that this reactive trajectory corresponds to the following process: initially, this molecule vibrates around the equilibrium geometry (region A). Then, the hydrogen atom connecting the carbon moves around the IRC during several vibrations and gradually approaches the transition state, which corresponds to the uphill motion on the potential energy surface along the IRC to the transition state (region B). Finally, this molecule exceeds the transition state and produces two fragments, CO and H_2O. Vibrational frequencies disappear around 550 and 600 fs, which corresponds to the downhill motion across the transition state to the product (region C). After 600 fs, almost constant frequencies appear; these correspond to the vibrational frequencies for two fragments, *i.e.*, H_2O and CO (region D). A similar situation may be explained for reaction (2) in Fig. 6(b). We cannot observe a clear picture for the movement

from the equilibrium geometry of the reactant to the transition state in this figure. A peak around 2000 cm^{-1}, which is assigned to a C=O stretching mode, increases slightly near the transition state; then, many frequencies disappear for a short time, which corresponds to the downhill motion. Finally, two fragments, CO_2 and H_2, are produced. From these figures, we concluded that the movements along the IRC observed by using the classical trajectory could be described by the ST-MEM.

The ST-MEM for a non-reactive trajectory is illustrated in Figs. 7(a) and (b). Note that sufficient excess energy required to exceed the transition state has been added to a specific vibrational mode. Compared with Fig. 4(a), the fluctuations of the vibrational modes become large due to the large internal vibrational energy. Contrary to Fig. 6, special features for the ST-MEM of the reactive trajectory are not observed; this corresponds to the uphill and downhill motions along the IRC and to the vibrational modes for fragments. It should be noted that the vibrational jumping does not necessarily suggest that a chemical reaction is taking place.

4. Conclusions

In the present paper, we studied the unimolecular decomposition of formic acid by using the classical trajectory calculation and discussed the reactivity of the two competitive channels semi-quantitatively. We also showed the ST-MEM spectra for the trajectory information of the decomposition of formic acid. Furthermore, we suggested that the

dynamics around the IRC could be resolved by analyzing the reactive trajectories. The ST-MEM is useful in elucidating the dynamics within the order of femto-seconds in the trajectory calculations for relatively large molecules. In order to understand the reaction mechanism in detail, more reactive trajectories need to be studied.

5. Acknowledgments

The authors thank the Information Media Center at Hiroshima University for the use of a grid with high-performance PCs and the Research Center for Computational Science, Okazaki, Japan for the use of a Fujitsu VPP5000 and PRIMEQUEST. This work was supported by a Grant-in-Aid for Scientific Research (B) (Contract No. 18350011) of the Ministry of Education, Culture, Sports, Science and Technology, Japan.

Table 1. The number of reacted trajectories per sixty runs in the case of the equilibrium structure as the starting point. (a) and (b) Z-formic acid for the initial geometry, and (c) and (d) E-formic acid.

(a) Z-HCOOH → $CO+H_2O$

E_{exc} / kcal mol^{-1}	ν_1	ν_2	ν_3	ν_4	ν_5	ν_6	ν_7	ν_8	ν_9	sum
5	0	0	0	1	0	0	0	1	0	2
10	1	0	0	0	0	3	0	4	1	9
15	2	1	5	4	0	1	5	9	0	27
sum	3	1	5	5	0	4	0	14	1	38

(b) Z-HCOOH → CO_2+H_2

E_{exc} / kcal mol^{-1}	ν_1	ν_2	ν_3	ν_4	ν_5	ν_6	ν_7	ν_8	ν_9	sum
5	0	0	0	0	0	0	0	0	0	0
10	0	0	0	0	0	0	0	0	0	0
15	1	1	0	0	0	0	0	0	0	2
sum	1	1	0	0	0	0	0	0	0	2

(c) E-HCOOH → $CO+H_2O$

E_{exc} / kcal mol^{-1}	ν_1	ν_2	ν_3	ν_4	ν_5	ν_6	ν_7	ν_8	ν_9	sum

5	0	1	0	1	0	4	0	1	0	7
10	0	4	4	1	0	4	1	2	1	17
15	0	12	3	1	0	11	9	7	2	45
sum	0	17	7	3	0	19	10	10	3	69

(d) E-HCOOH → CO_2+H_2

E_{exc} / kcal mol^{-1}	ν_1	ν_2	ν_3	ν_4	ν_5	ν_6	ν_7	ν_8	ν_9	sum
5	0	0	0	0	0	0	0	0	6	6
10	0	0	0	0	0	0	0	0	7	7
15	2	0	0	1	0	2	0	0	12	17
sum	2	0	0	1	0	2	0	0	25	30

Figure captions

Fig. 1 Potential energy diagram of the decomposition of formic acid. Relative energies at the MP2/6-31G(d,p) level are shown. Relative energies at the MP4/cc-pVQZ//B3LYP/cc-pVTZ level are shown in parentheses.

Fig. 2 Comparison of the power spectra obtained by FT with those obtained by MEM.

Fig. 3 ST-MEM spectrum of formic acid with zero-point energy. A window function of 500 fs was applied.

Fig. 4 Spectrograms of formic acid with zero-point energy. Window functions of (a) 500 fs and (b) 100 fs were applied.

Fig. 5 Spectrograms immediately after mode specific excitation for a specific trajectory. (a) mode ν_6, which is assigned to a CH rocking mode, and (b) mode ν_5, which is assigned to a COH bending mode.

Fig. 6 Spectrograms for a reactive trajectory. (a) Excess energy was added to mode ν_3 for Z-HCOOH, and reaction (1) occurred. (b) Excess energy was added to mode ν_6 for E-HCOOH, and reaction (2) occurred.

Fig. 7 Spectrograms for a non-reactive trajectory. (a) Excess energy was added to mode ν_3 for Z-HCOOH. (b) Excess energy was added to mode ν_9 for E-HCOOH.

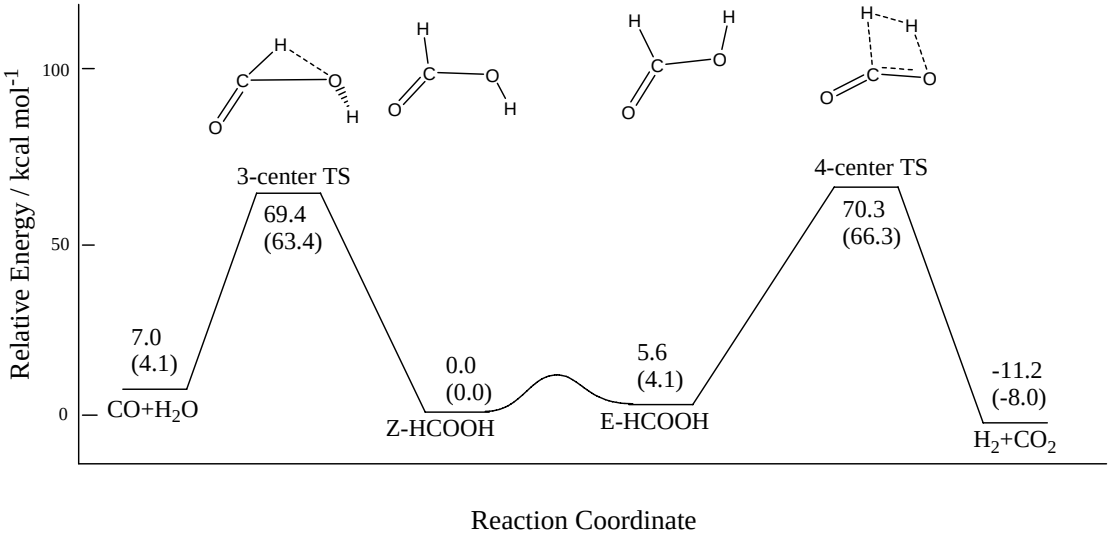

Fig. 1 Takahashi et al.

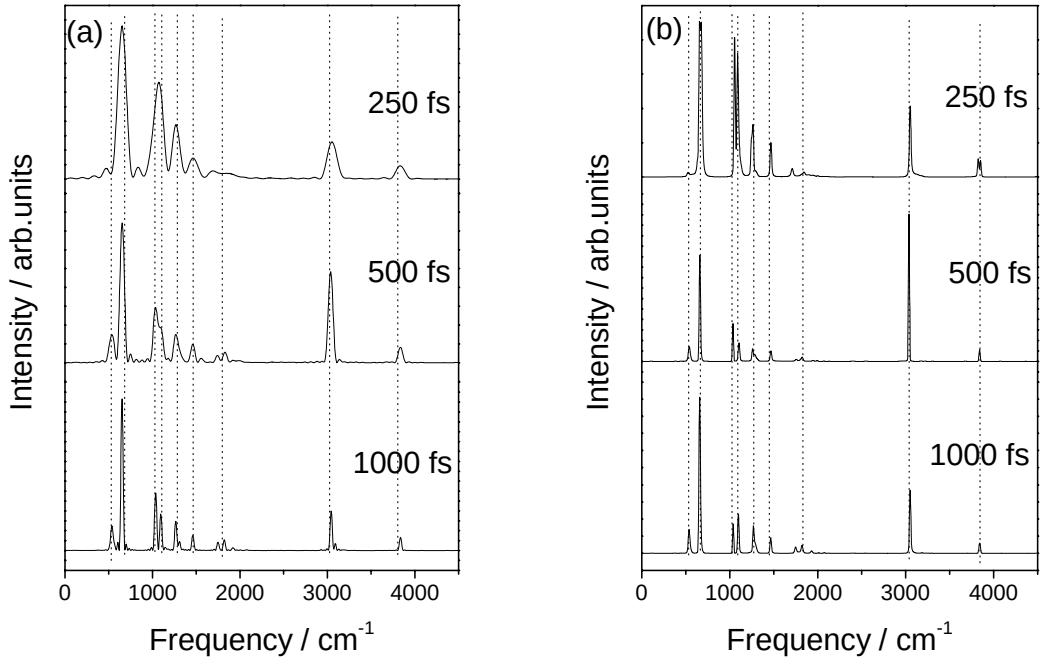

Fig. 2 Takahashi et al

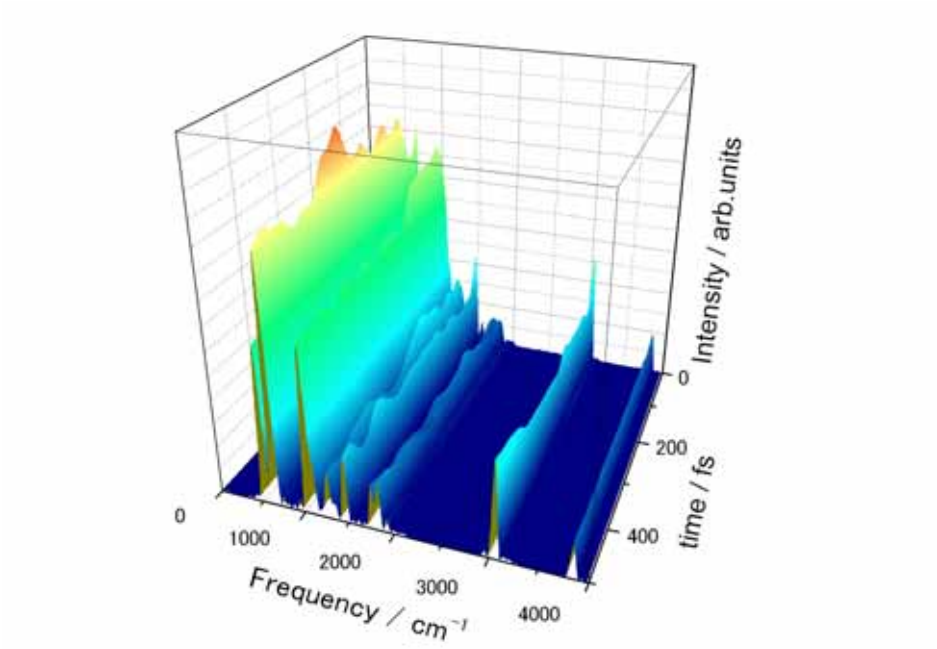

Fig. 3 Takahashi et al.

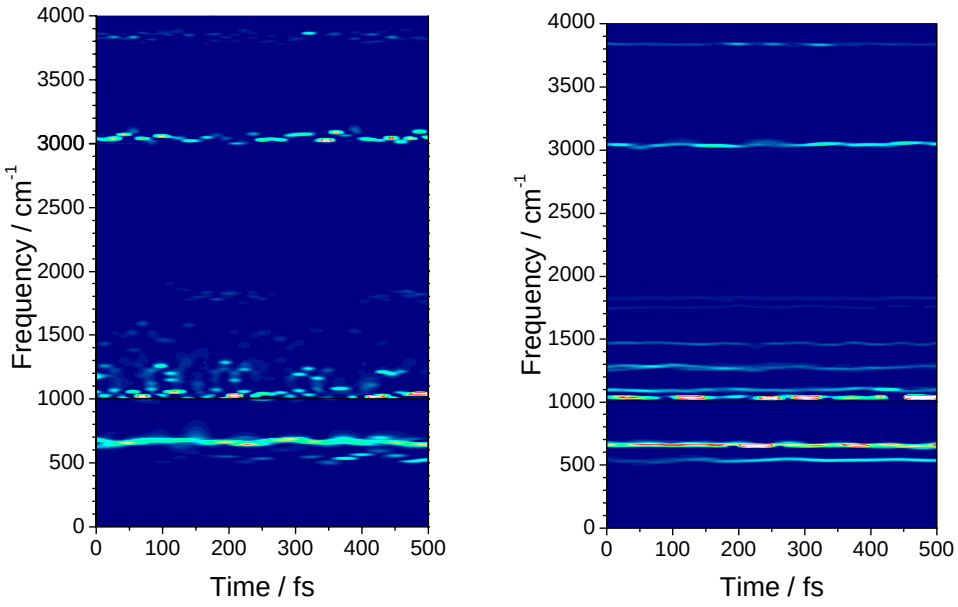

(a) (b)

Fig. 4 Takahashi et al.

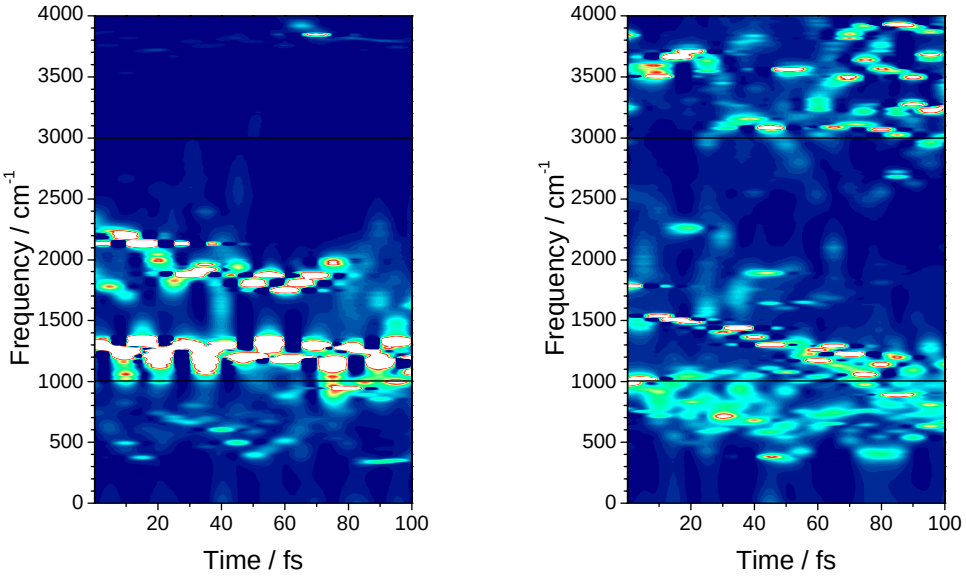

Fig. 5 Takahashi et al.

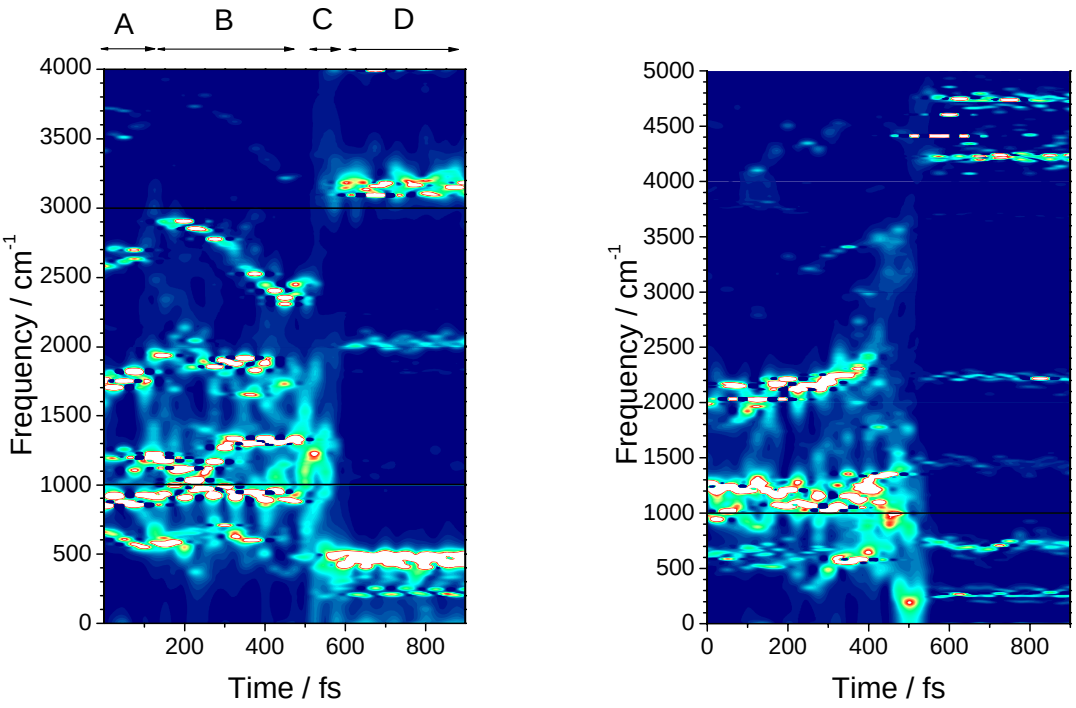

Fig. 6 Takahashi et al.

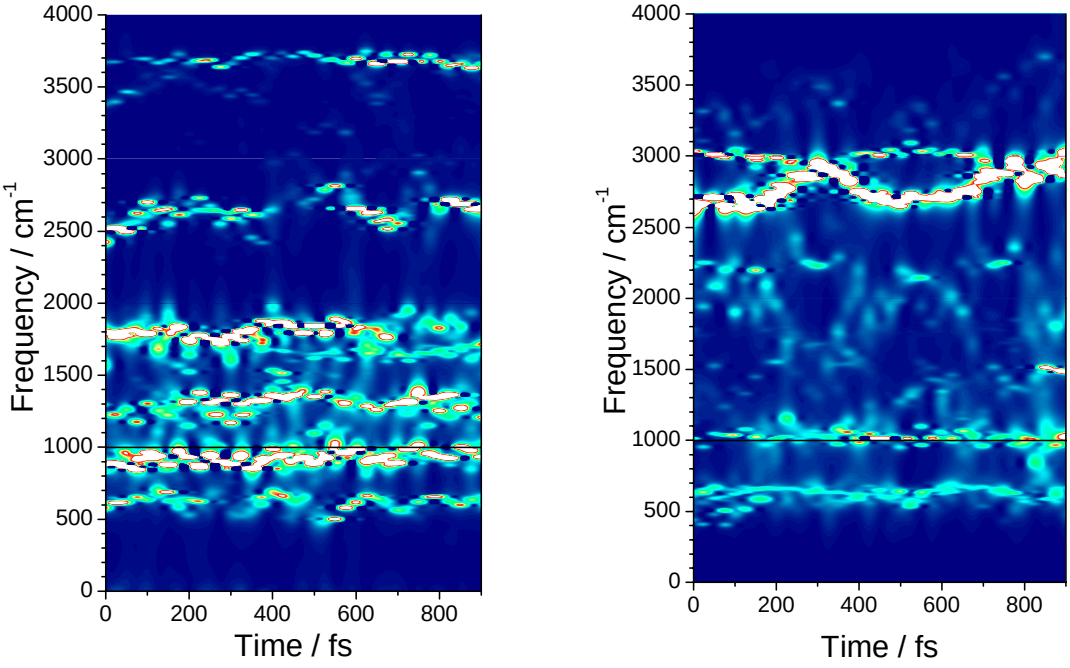

(a) (b)

Fig. 7 Takahashi et al.

References

[1] AH Zewail, J. Phys. Chem. A 104 (2000) 5660.
[2] K Ohmori, Y Sato, EE Nikitin, SA Rice, Physical Review Letters 91 (2003).
[3] O Takahashi, M Odelius, D Nordlund, H Bluhm, A Nilsson, LGM Pettersson, J. Chem. Phys. 124 (2006) 064307.
[4] M Odelius, H Ogasawara, D Nordlund, O Fuchs, L Weinhardt, F Maier, E Umbach, C Heske, Y Zubavichus, M Grunze, JD Denlinger, LGM Pettersson, A Nilsson, Phys. Rev. Lett. 94 (2005) 227401.
[5] DW Noid, ML Koszykowski, RA Marcus, J. Chem. Phys. 67 (1977) 404.
[6] XY Chang, TD Sewell, LM Raff, DL Thompson, J. Chem. Phys. 97 (1992) 7354.
[7] PJ Stimac, JR Barker, Journal of Physical Chemistry A 110 (2006) 6851.
[8] Y Yamauchi, S Ozawa, H Nakai, Journal of Physical Chemistry A 111 (2007) 2062.
[9] Y Yamauchi, H Nakai, Journal of Chemical Physics 123 (2005) 034101/1.
[10] M Tamaoki, Y Yamauchi, H Nakai, Journal of Computational Chemistry 26 (2005) 436.
[11] Y Yamauchi, H Nakai, Y Okada, Journal of Chemical Physics 121 (2004) 11098.
[12] A Rahaman, RA Wheeler, J. Chem. Theo. Comp. 1 (2005) 769.
[13] T Otsuka, H Nakai, Journal of Computational Chemistry 28 (2007) 1137.
[14] JP Burg, Maximum entropy spectral analysis,, the 37th Annual International Meeting, Soc. of Explor. Geophys., Oklahoma City, 1967.
[15] JP Burg, A new analysis technique for time series data, Advanced Study Institute on Signal Processing, Enschede, Netherlands, 1968.
[16] M Andersen, Geophysics 39 (1974) 69.
[17] WH Press, SA Teukolsky, WT Vetterling, BP Flannery, Numerical recipes in Fortran 77, Cambridge University Press, Cambridge, 1992.
[18] PG Blake, CH Sir, Proc. R. Soc. London Ser.A 255 (1960) 444.
[19] PG Blake, HH Davies, G Jackson, J. Chem. Soc. (1971) 1923.
[20] R Corkum, C Willis, RA Back, Chem. Phys. 24 (1977) 13.
[21] DS Hsu, WM Shaub, M Blackbrun, MC Lin, The Ninteenth International Symposium on Combustion, 1983.
[22] K Saito, T Kakumoto, H Kuroda, S Torii, A Imamura, J. Chem. Phys. 80 (1984) 4989.
[23] K Saito, T Shiose, O Takahashi, Y Hidaka, F Aiba, K Tabayashi, Journal of Physical Chemistry A 109 (2005) 5352.
[24] O Takahashi, K Itoh, A Kawano, K Saito, J. Mol. Struct. THEOCHEM 545 (2001) 197.
[25] K Yamashita, T Yamabe, Int. J. Quantum Chem. Symp. 17 (1983) 177.
[26] P Ruelle, UW Kesselring, Hh Nam-Tran, J. Am. Chem. Soc. 108 (1986) 371.
[27] P Ruelle, J. Am. Chem. Soc. 109 (1987) 1722.
[28] J Lundell, M Rasanen, Z Latajka, J. Phys. Chem. 97 (1993) 1152.

[29] YT Chang, Y Yamaguchi, WH Miller, IHF Schaefer, J. Am. Chem. Soc. 109 (1987) 1330.
[30] I Yokoyama, Y Miwa, K Machida, J. Am. Chem. Soc. 113 (1991) 6458.
[31] JD Goddard, Y Yamaguchi, HFS III, J. Chem. Phys. 96 (1992) 1158.
[32] JS Francisco, J. Chem. Phys. 96 (1992) 1167.
[33] IV Tokmakov, CC Hsu, LV Moskaleva, MC Lin, Mol. Phys. 92 (1997) 581.
[34] N Akiya, PE Savage, AiChE J. 44 (1998) 405.
[35] E Martinez-Nunez, S Vazquez, G Granucci, M Persico, CM Estevez, Chemical Physics Letters 412 (2005) 35.
[36] Y Kurosaki, K Yokoyama, Y Teranishi, Chemical Physics 308 (2005) 325.
[37] H Yoshida, Phys. Lett. 150 (1990) 262.
[38] O Takahashi, N Kurushima, A Kawano, K Saito, Chem. Phys. Lett. 338 (2001) 398.
[39] MW Schmidt, KK Baldridge, JA Boatz, ST Elbert, MS Gordon, JH Jensen, S Koseki, N Matsunaga, KA Nguyen, SJ Su, TL Windus, M Dupuis, JA Montgomery, Journal of Computational Chemistry 14 (1993) 1347.